Overview

Residual stress
Part 2 – Nature and origins

P. J. Withers and H. K. D. H. Bhadeshia

Residual stress is that which remains in a body that is stationary and at equilibrium with its surroundings. It can be detrimental when it reduces the tolerance of the material to an externally applied force, as is the case with welded joints. On the other hand, it can be exploited to design materials or components which are resistant to damage, toughened glass being a good example. This paper, the second part of a two part overview, the first part having been devoted to measurement techniques, examines the nature and origins of residual stresses across a range of scales. This extends from the long range residual stress fields in engineering components and welded structures, through the interphase stresses present in composites and coatings, to the microscale interactions of phase transformations with local stresses. **MST/4640B**

Professor Withers is in the Manchester Materials Science Centre, University of Manchester and UMIST, Grosvenor Street, Manchester M1 7HS, UK (philip.withers@man.ac.uk). Professor Bhadeshia is in the Department of Materials Science and Metallurgy, University of Cambridge, Pembroke Street, Cambridge CB2 3QZ, UK (hkdb@cus.cam.ac.uk). *Manuscript received 3 March 2000; accepted 6 December 2000.*
© 2001 IoM Communications Ltd.

Introduction

As the design of engineering components becomes less conservative, there is increasing interest in how residual stress affects mechanical properties. This is because structural failure can be caused by the combined effect of residual and applied stresses. In practice, it is not likely that any manufactured component would be entirely free from residual stresses introduced during processing. Furthermore, in natural or artificial multiphase materials, residual stresses can arise from differences in thermal expansivity, yield stress, or stiffness.

As discussed in part 1,[1] residual stresses arise from misfits in the natural shape between different regions (as in shot peening), different parts (such as the stresses around a rivet in a plate), or different phases (as is the case for composites). The terminology for describing these is given in detail in part 1. In essence, the stresses can be discussed in terms of their characteristic length,[2] l_0, which is the length over which the stresses equilibrate. Long range stresses (type I) equilibrate over macroscopic dimensions ($l_{0,I} \approx$ the scale of the structure). Such stresses can be estimated using continuum models which ignore the polycrystalline or multiphase nature of the material, often calculated using finite elements. Type II residual stresses equilibrate over a number of grain dimensions ($l_{0,II} \approx 3-10 \times$ grain size). An example of these is the interphase thermal stresses in a metal matrix composite. Type III stresses, on the other hand, exist over atomic dimensions and balance within a grain ($l_{0,III} <$ grain size), for example, those caused by dislocations and point defects.

The materials technologist has a plethora of techniques of differing capability with which to characterise residual stress.[1] The challenge is to use information gained with these techniques in the optimisation and management of the residual stress state with the goal of improved processing and component design. In this paper, part 2 of the overview, the nature and origins of residual stress across a range of scales are examined, from the short range stresses typical of composite materials and phase transformations to longer range stresses in thin films, welds, and engineering structures.

Macro residual stresses in engineering components

There are at least four ways in which macro residual stresses can arise in engineering components: through the interaction between misfitting parts within an assembly, and through the generation of chemical, thermal, and plastically induced misfits between different regions within one part.

Whether the stresses acting between two or more misfitting parts are regarded as residual depends largely on the perspective. By way of an example, consider two plates riveted together. If either plate is considered separately, then the clamping stress exerted by the rivet is an externally applied stress. However, if one considers the complete riveted assembly, then the stresses are residual and must be added to any applied stresses it might experience in service. Misfits can also be generated chemically, thermally, or by plastic deformation. Nitriding is an example of the first type, whereby nitrides form in the surface of a steel with an associated volume increase. An example of thermal stress is provided by a shrink fit plug used as a 'round robin' standard for the assessment of neutron diffraction strain measurement facilities as part of the Versailles Agreement on Measurements and Standards working group TWA20.[3] The specimen was formed by inserting an oversized plug into a hole by cooling it before placement. The strain field is shown in Fig. 1. Thermal misfit stresses are commonly found in multipart assemblies comprising different materials which experience varying temperatures from electronic assemblies to space structures. Prestressed concrete and bolted structures are examples of macrostresses caused by mechanical means.

There are many examples of single piece structures for which internal stresses have been generated by thermal misfits between different regions. For example, the failure strength of glass is often improved by rapid cooling of the surface to create a compressive state of stress in the exterior and a tensile stress in the interior. Thermal stresses in glass objects can be studied non-destructively by photoelastic examination, a method often employed to examine large glass pots and sculptures which have been cooled very slowly to avoid cracking.

 ISSN 0267–0836

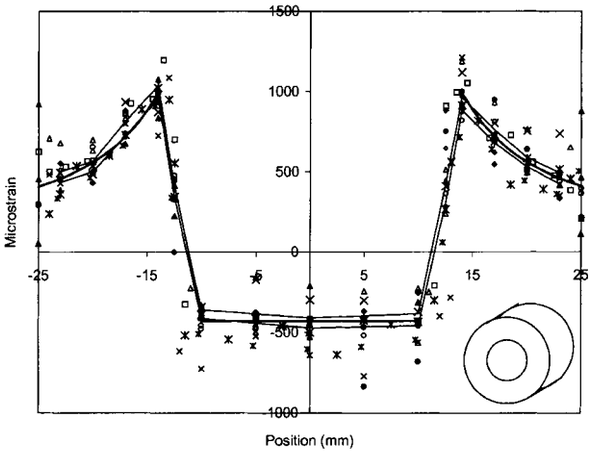

1 Strain field measured for Al ring and plug (supplied by T. Holden, AECL, Canada): in total over ten neutron facilities took part in 'round robin' and between them showed standard deviation of ±75 microstrain (analytical solution is also shown as central solid line)[3]

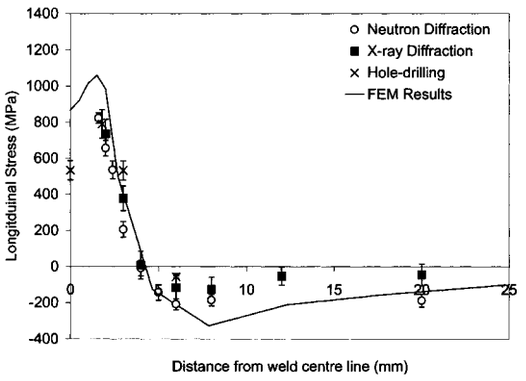

2 Residual stress longtudinal to electron beam weld in Ni superalloy measured by neutron diffraction (data averaged over 0·3 mm located just below surface), X-ray diffraction (data averaged over ~10 μm from surface), and hole drilling (data averaged over 1 mm): finite element analysis (FEM) is also shown for comparison[4]

Another area of great technological importance is welding. In this case, large thermal stress gradients are caused in the vicinity of welded joints by the localised heating and subsequent cooling of the weld zone (Fig. 2). This contraction can cause weld cracking or distortion during welding, leading to non-conformance rejection or reduced service life. Welded structures can as a consequence become susceptible to hydrogen embrittlement and other detrimental phenomena. Residual stresses can be especially problematic given the tendency for stress concentration at joints and the possibility of detrimental microstructures in the heat affected zone of the weld. Residual stress measurements are particularly important for the introduction of new joining processes, such as electron beam welding,[4] inertia welding,[5] laser thermally tensioned tungsten inert gas welding,[6] and friction stir welding,[7] into commercial usage. Measurements are helping with lifing, the development of postweld heat treatments, and the validation of finite element process models for process optimisations to minimise detrimental residual stresses and distortion. In this respect, depth scanning methods such as neutron diffraction are particularly useful because they produce three-dimensional stress or strain maps for direct comparison with finite element output.

Another important means of generating macro residual stresses is by non-uniform plastic deformation. For example, shot peening[8,9] and grinding[9] can cause large compressive surface stresses which fall off rapidly with increasing depth into the body (Fig. 3).[10–13] The plastic bending of a bar is a simple way of introducing residual stresses which vary over the whole thickness of the bar. Industrial examples include autofrettaging of cylinders[8] and gun barrels,[8] overspeeding of rotating discs,[8,14] prestressing of springs, and overloading to reduce weld stresses in pressure vessels.[15] The principle behind many of these treatments is to yield the component in the same direction as anticipated in future loading to produce plastic misfits, and hence residual stress fields that will minimise future yielding. By way of an example, consider the autofrettaging of thick cylinders by internal pressurisation. As the internal pressure is raised, the inner diameter exceeds the yield strength. The plastic zone penetrates deeper into the cylinder wall with increasing pressure. When the pressure is released, the outer elastic portion attempts to return to its original state but is prevented from doing so by the tensile hoop plastic misfit strain that has been introduced into the inner portion. As a result the outer elastic region is maintained in residual hoop tension, while the inner portion is in compression. In some cases, numerical methods must be used to compute the residual stresses, but in others, as is the case here, analytical solutions are available.[8,14] As an illustrative example, consider autofrettage of a cylinder made of material having a yield strength σ_y and having inner and outer radii R_1 and R_2 with the plastic zone extending to R_p. The internal pressure P_A required to do this, assuming a Tresca yield criterion, is given by

$$P_A = \sigma_y \left(\ln \left\{ \frac{R_p}{R_1} \right\} + \frac{1}{2} \left[1 - \frac{R_p^2}{R_2^2} \right] \right) \quad . \quad . \quad . \quad . \quad . \quad . \quad (1)$$

The maximum autofrettage pressure allowed by the High Pressure Technology Association Code of Practice is that which extends the plastic zone to the geometric mean radius $(R_1R_2)^{1/2}$. The hoop stresses σ_H in the plastic zone and elastic zone vary as a function of the radial position according to

$$\sigma_H = \sigma_y \left(1 + \ln \left\{ \frac{R}{R_p} \right\} - \frac{1}{2} \left[1 - \frac{R_p^2}{R_2^2} \right] \right) \quad . \quad . \quad . \quad . \quad (2a)$$

and

$$\sigma_H = \frac{P_p R_p^2}{R_2^2 - R_p^2} \left[1 + \frac{R_p^2}{R^2} \right] \quad . \quad . \quad . \quad . \quad . \quad . \quad . \quad . \quad . \quad (2b)$$

respectively, where P_p is the pressure at the interface between the plastic and elastic zones during autofrettaging and is given by $\sigma_y(R_2^2 - R_p^2)/2R_2^2$. To calculate the residual stress, the stress change caused by unloading elastically must be superimposed upon either the elastic or plastic stress above according to the location. This change is given simply by replacing P_p by $-P_A$ and R_p by R_1 in the elastic loading equation above. In the case illustrated in Fig. 4, the in-service load is insufficient to reverse the compressive stress near the bore and so it is not surprising that a significant increase in life is achieved by this pretreatment.[16,17] Neutron diffraction[18,19] and material removal methods[20] are well suited to evaluating stresses due to autofrettaging, and other cases involving plastically introduced long range stresses.

On the whole, surface methods of stress measurement are not well suited to the measurement of macro residual stresses because the surface stress is often an unreliable indicator of the body as a whole. On the other hand, destructive near surface methods such as hole drilling and X-ray diffraction (with layer removal) can often be

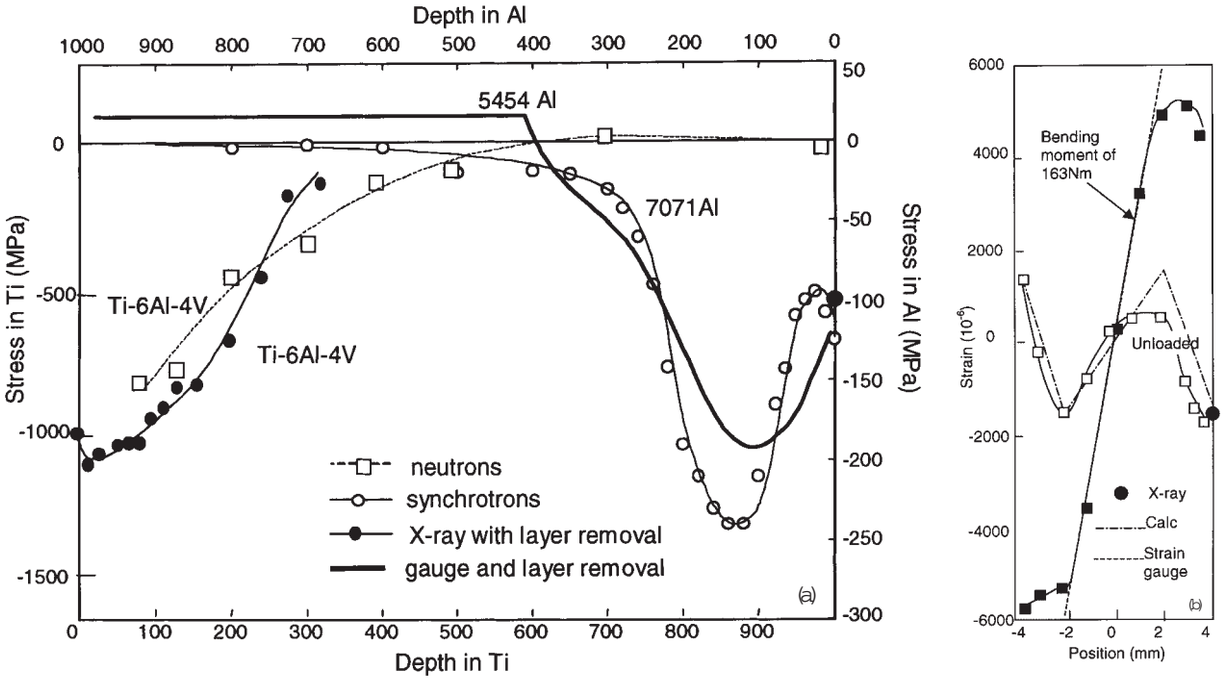

a residual stress in shot peened samples, as measured by layer removal, neutron, X-ray, and synchrotron X-ray diffraction;[10–12] *b* variation in residual stress caused by plastically bending Al bar determined by X-ray diffraction and layer removal[13]

3 Macro residual stresses generated by non-uniform plastic deformation

considered non-destructive for large objects such as thick pressure vessels. In such circumstances, reliable measurements can be obtained provided there is sufficient understanding to infer the overall state of stress. Of course, the bulk methods are especially useful for macrostress measurement and, because the characteristic length l_0 is usually large, spatial resolution is not normally a problem. Provided the penetration distance is not too great ($\sim$2·5 cm for steel) or the specimen too large ($>$200 kg), neutron diffraction is an effective, if somewhat expensive non-destructive technique for crystalline materials. Photoelasticity is suited to transparent glasses and polymers, while magnetic methods can provide a quality inspection technique for ferritic steels. For welded structures, microstructural changes can complicate the interpretation of the magnetic response, while changes in the stress free lattice spacing as a function of thermal history in the weld zone requires stress free references for neutron diffraction. Ultrasonic studies can provide information at depth, for example, during bolt tensioning.[21] Full three-dimensional sectioning is a simple, but time consuming method of determining the stress state in situations where non-destructive testing is not required.[22]

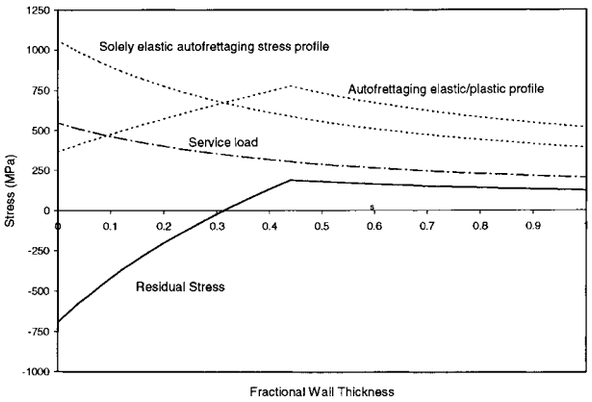

4 Stress field predicted during and after autofrettaging cylinder (i.d. 178 mm, o.d. 373 mm, assumed σ_Y of 1035 MPa) to internal pressure of $\sim$660 MPa causing plastic zone to extend to $\sim$45% of wall thickness (45% overstrained): these conditions correspond to those found in practice significantly to extend life of US Army gun barrels that experience internal pressure of 345 MPa during each firing[16,17]

Thin films and coatings

Thin films and coatings are used for applications ranging from corrosion and wear protection to aiding biocompatibility. Residual stresses are almost always present and may prove life limiting leading to cracking or spalling, or they may degrade performance. Curvature and X-ray residual stress evaluation methods are most commonly applied,[23] although other methods such as Raman spectroscopy have also been used.[24]

Stresses in thin films are divided into two types: extrinsic, such as stresses arising from a mismatch in thermal expansion coefficients, and intrinsic, such as stresses arising from coherent epitaxial deposition.[25] Differential thermal contraction stresses are an unavoidable consequence of processing at elevated temperature and can become quite large because coating and substrate often have very different thermal expansion characteristics. For example, for a 10 mm steel/1 mm alumina system, compressive coating stresses as high as 70 MPa are generated for a 100 K temperature change.[26] Such stresses are fairly easily calculated in process models. Of course, the deposition process itself may introduce residual stresses, for example, chemical vapour deposition can give rise to compressive or tensile coating stresses[27] depending on the conditions, whereas plasma deposition always gives rise to tensile deposit stresses as the individual splats cool on the substrate; these can be as high as 300 MPa.[28] Compressive stresses (as large as 70 MPa) have long been exploited in ceramic glazes used to protect items of pottery.

Relaxation processes, such as plastic flow, creep, and microcracking, can act to reduce coating stress. This, combined with the fact that their extent may vary as a function of depth, can complicate the prediction of coating stress. Furthermore, it can often be difficult to determine the elastic properties of thin coatings, let alone the required inelastic ones, especially for complex multicoated systems, such as the (ceramic) thermal and (MCrAlY) bond coated systems used to protect single crystal nickel superalloy turbine blades.

The measurement of stresses in thin films by the measurement of curvature of narrow strips (Fig. 4, part 1[1]) usually relies on the modified Stoney formula[29]

$$\sigma_{\text{film}} = \frac{Et_0^2(K-K_0)}{6(1-v)t} \qquad (3)$$

where E is Young's modulus, t_0 is the substrate thickness, t is the film thickness, K is the curvature of the coated substrate, K_0 is the curvature of the uncoated substrate, and v is Poisson's ratio. For thicker films, stress gradients in both film and substrate are important. In such cases, assumptions about the coating/substrate misfit must be made to interpret post-mortem curvature measurements in terms of stress distributions without layer removal. Stresses have been characterised for thermally sprayed coatings,[26] thermal barrier coatings,[30] hydroxyapetite biocompatible coatings,[31,32] and sputtered thin films[33] by curvature methods.

The measurement of stresses in thin films by X-ray methods has been excellently reviewed by Noyan *et al.*,[25] but can be broadly categorised into the conventional $\sin^2\psi$, glancing and grazing incidence methods. These have been described in part 1,[1] and are applied in turn to progressively thinner coatings. The $\sin^2\psi$ method has been very widely applied to relatively thick ($>0{\cdot}5$ μm) thin films,[25,34] e.g. diamond-like films,[35] chemical vapour deposition of silicon films,[36] hydroxyapetite films,[37] and thermal barrier coatings.[34] Problems include peak broadening for very fine grained coatings, loss of peak intensity as ψ is varied for very textured coatings, and the depth of penetration (some tens of micrometres) which can be on a scale equal to the surface roughness for thick coatings.

In a comparison of curvature and X-ray methods of stress evaluation in sputtered molybdenum thin films, Malhotra *et al.*[33] found that the curvature methods provided lower estimates of stress. This was ascribed to the fact that the former measures the extrinsic stresses while the latter may be influenced by intrinsic stresses or texture effects, which is in agreement with comments made by Noyan *et al.*[25]

Multilayers are in many respects similar to thin films in that the layer thickness can be comparable, and the deposition processes are often the same. However, in this case, curvature methods are not usually appropriate as stresses between alternate layers may balance and thus may not lead to any bending of the multilayer as a whole. As to whether X-ray diffraction provides a measure of the stress in the top layer only, or an average over many layers, that depends largely on the layer thickness. For example, in micrometre and submicrometre layer thickness Cu–Ni electrodeposited multilayers $l \gg l_{0,\text{II}}$ so that an average over a number of copper or nickel layers was obtained by the conventional $\sin^2\psi$ method.[38]

Composite and multiphase materials

Composites are designed to unite the contrasting merits of two or more different phases. For example, the stiffness of a brittle ceramic reinforcement might be combined with a compliant plastically deformable matrix. As a result, composites are intrinsically heterogeneous, their performance depending upon the generation of an uneven partitioning of the applied stresses, i.e. on the generation of large type II mean phase microstresses.

In general, the microstructures of most composites are fine so that the characteristic length $l_{0,\text{II}}$, which is approximately equal to the structural spacing in the relevant direction,[1] is short. Few methods are thus able to resolve the local variation in stress between the phases. For composites in which either the matrix or fibres fluoresce or give Raman spectra, piezospectroscopic methods can be used having a spatial resolution of about 1 μm.[39] In addition, synchrotron X-ray diffraction can achieve a lateral spatial resolution of 20 μm.

While the characterisitic volumes associated with most diffraction techniques are generally considerably larger than $V_{0,\text{II}}$, their phase specificity does allow the measurement of type II mean stresses in matrix $\langle\sigma_M\rangle_i^{II}$ and reinforcement $\langle\sigma_R\rangle_i^{II}$, where the subscripts represent matrix and reinforcement respectively and i indicates the tensor component. As shown in part 1,[1] they are related by

$$(1-f)\langle\sigma_M\rangle_i^{II} + f\langle\sigma_R\rangle_i^{II} = 0$$

Neutron diffraction in particular has provided a great deal of information about thermal and load induced stresses.[40] As regards X-ray diffraction, a problem of interpretation can arise if attempting to apply the conventional $\sin^2\psi$ technique. If the reinforcement spacing is coarser than the incident penetration (i.e. $l \ll l_{0,\text{II}}$) the stress state is very unrepresentative of the bulk type II stresses. If, on the other hand, the penetration is much greater than the spacing (i.e. $l \gg l_{0,\text{II}}$) then the bulk state is sampled. For particulate composites $\langle\sigma_M\rangle_{\text{normal}}^{II} - \langle\sigma_M\rangle_{\text{in-plane}}^{II} = 0$ so that the $\sin^2\psi$ gradient is zero. Ordinarily this is indicative of zero stress. In this case, satisfactory results can be obtained only if the three-dimensional stress measurement technique is followed.[41] At intermediate penetration, non-linearities in the $\sin^2\psi$ curve can give confusing results.

Diffraction methods can even be used to good effect for amorphous polymer matrix systems provided a crystalline marker (a compliant crystalline material is best for good sensitivity) is included in the composite.[42] Synchrotron diffraction is particularly well suited, having high penetration (many millimetres) in contrast to X-rays, and high spatial resolution compared to neutron diffraction. Finally, in systems containing coarse fibres (>10 μm) it has proven possible to use etchant/relaxation methods to assess fibre strains.[43]

A wide variety of models have been proposed to predict the internal stresses and the resulting performance of composites. The majority fall in to one of two categories: Eshelby derived analytical models[44,45] and finite element numerical models.[46] The former have the advantage that they can be computed using a spreadsheet, and allow a clear visualisation of the load transfer mechanisms; however, they are generally better at predicting mean phase stresses rather than detailed stress fields. The latter have the advantage that complex constitutive laws and various fibre shapes/arrangements can be modelled, but in most cases they require an idealised unit cell representing, what is in reality, a more chaotic distribution. While the full stress fields are useful for studying phenomena such as fibre debonding and cracking, the results are fibre arrangement specific and it is difficult to obtain validatory stress measurements due to insufficient spatial resolution of the measurement techniques for all but the coarsest systems. Despite this, researchers tend to show pictures of stress contours rather than quote the mean phase stress values, prohibiting direct comparison with experiment.

THERMAL STRESSES

Thermal microstresses often arise because the composite fabrication temperature is rarely the envisaged use temperature and the composite phases seldom have the same

coefficients of thermal expansion. This is true of ceramic matrix composites which are usually hipped at elevated temperature,[47] of metal matrix composites which are usually fabricated either in the melt, or at temperatures sufficient for significant diffusion to occur,[46] and of thermoplastic matrix composites which are also processed in the melt. Thermoset matrix systems are usually residually stressed due to a combination of changing temperature and stresses introduced by curing contraction during manufacture.[48]

A commonly used concept for describing the thermal stress state is that of the effectively stress free temperature T_{esf}. This is not the temperature at which there were no stresses present in the composite, but that from which the composite would need to be cooled to reproduce the actual thermal stresses if the thermal expansion misfit $\Delta\alpha\Delta T$ between the phases were the misfit accommodated elastically. In the notation of part 1,[1] the type II mean phase thermal stresses can be estimated using Eshelby's approach[44] or by finite element analysis

$$\langle\sigma_M\rangle_i^{II} = B_{M_{ij}}\Delta\alpha_j\Delta T_{esf} \quad \ldots\ldots\ldots \quad (4a)$$

and

$$\langle\sigma_R\rangle_i^{II} = B_{R_{ij}}\Delta\alpha_j\Delta T_{esf} \quad \ldots\ldots\ldots \quad (4b)$$

where $\Delta\alpha\Delta T_{esf}$ is the effective thermal expansion misfit which is accommodated elastically. The parameters $B_{R_{ij}}$ and $B_{M_{ij}}$ reflect the influences of reinforcement volume fraction, phase stiffnesses, and phase geometry on the level of internal stress generated per unit thermal expansion misfit. These have been calculated for Al/SiC using the Eshelby method in Ref. 49. In many cases, $\Delta\alpha$ is a strong function of temperature, in which case the accumulated misfit must be calculated by integration over the relevant temperature range. Of course, the stress free temperature reflects the opportunities for the relaxation of the misfit by creep and yielding at high temperatures and yielding, cracking, debonding, etc. at low temperatures. Most mean phase thermal microstress measurements have been made by neutron or X-ray diffraction.[40] Effective stress free temperatures of about 250, 700, and 1300°C are typical of aluminium,[50] titanium,[51] and alumina[52] matrix systems.

PLASTICALLY INDUCED STRESSES

Plastically induced mean phase microstresses are those caused by plastic misfit generated due to incompatabilities in plastic straining between matrix and reinforcement. They often arise in composites comprising a ductile metal matrix and elastically deforming ceramic reinforcement. They are essentially shape misfit stresses analogous to those generated by thermal expansion mismatches or shape changing transformations. They differ from the above cases because the misfits need not be uniform in either phase, making it non-trivial to relate the internal stresses to the macroscopic plastic strain of the composite. The Eshelby based approach has been used to simplify this situation by assuming that the misfit strain between the phases is uniform, under which conditions the mean phase microstresses can be written as

$$\langle\sigma_M\rangle_i^{II} = B_{M_{ij}}\Delta\varepsilon_j^p \text{ and } \langle\sigma_R\rangle_i^{II} = B_{R_{ij}}\Delta\varepsilon_j^p \quad \ldots\ldots \quad (5)$$

Values of B are given in Ref. 53. Finite element models do not require such simplifying assumptions and an example of this approach is provided by Lorca *et al.*[54]

LOCAL STRESSES

As stated above, few techniques have a characteristic measurement volume smaller than $V_{0,II}$ typical of composite systems. Raman and flourescence techniques are exceptions, which although limited to near surface regions, have provided valuable insights about point to point variations

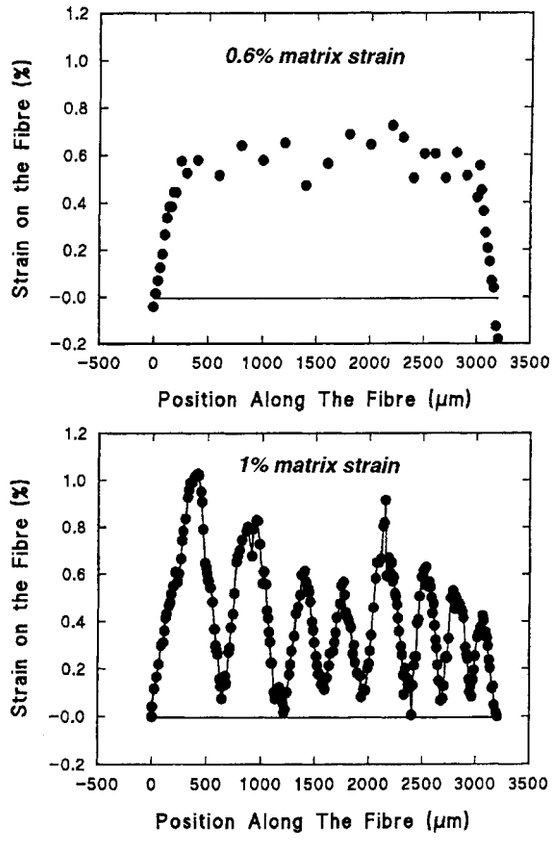

5 Variation of stress along C fibre in epoxy matrix as determined using Raman spectroscopy during full fragmentation test as loading proceeds[55]

in stress at the micrometre and submicrometre scale (Fig. 5). An alternative approach has been to interpret diffraction peak shapes in terms of the distribution of type II microstrains present.[52,56]

A recent experiment by Maire *et al.*[57] has exploited the high penetration, intensity, and spatial resolution of synchrotron radiation to map the build up of stress during loading of individual SiC fibres in a titanium matrix as a function of loading. Using a 100×200 μm beam, it was possible to scan the matrix and individual fibre strains as a function of distance from the fibre ends (Fig. 6). Note the initial tensile (matrix) and compressive (fibre) residual strains, the build up of tensile strain from the fibre end as the load is increased, and the effect of the fibre break.

Residual stress and phase transformations

TRANSFORMATION STRAINS

Phase changes are associated with transformation strains due to the change in crystal structure.[58] The strains are defined with respect to the stress free (unconstrained) transformation.[59] They may be accommodated in a variety of ways when, as is usual, the transformation product is constrained by the surrounding matrix phase. Irrespective of the details of the process of accommodation, the very existence of strains means that the transformations can be regarded as modes of deformation with the special characteristic that the deformation is accompanied by a change in the crystal structure.[60] It is natural, therefore, that they should contribute to the evolution of residual stresses.[61–69]

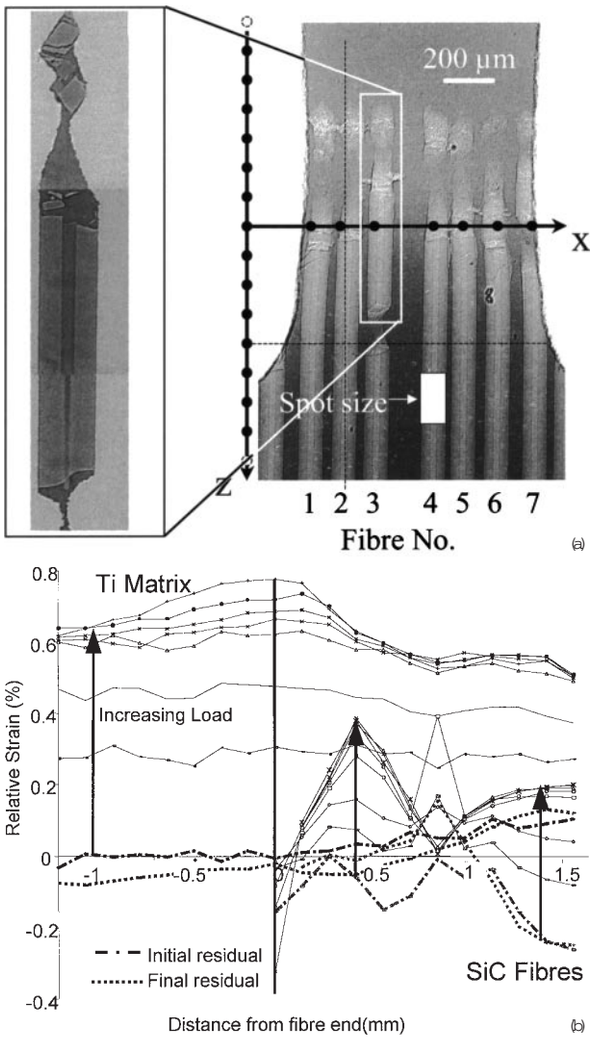

a radiograph and tomographic section (inset) taken on ID19 of composite after unloading just before failure; *b* longitudinal fibre and matrix strains as function of fibre position for fibre 3 in *a* measured by synchrotron radiation in ID11 at European Synchrotron Research Facility

6 Relationship between damage and load in Ti/SiC fibre composites[57]

Transformations occur in two main ways:[70] the displacive mechanism, in which the new structure is produced by a deformation of the parent crystal, and reconstructive transformation, involving the uncoordinated diffusion of all of the atoms, including those of the host lattice. Both are usually accompanied by substantial strains; some typical value are given in Table 1. The reconstructive transformations cause a volume change which is, in general, isotropic (Fig. 7*a*), whereas displacive transformations involve a combination of a shear on the habit plane and a dilatational strain which is directed normal to the habit plane. The strain associated with displacive transformations is known as an invariant-plane strain (IPS) because it leaves the habit plane undistorted and unrotated (Fig. 7).[70,72] Table 1 shows that the transformation strains can be very large, greatly exceeding elastic strains which are generally of the order of 10^{-3}.

TRANSFORMATION MICROSTRESSES – MACROSTRESS INTERACTIONS

Residual stresses due to transformations are often introduced unintentionally during fabrication and can have a large effect on the residual stresses that would otherwise occur. Jones and Alberry[73,74] conducted an elegant series of experiments to illustrate the role of transformations on the development of residual stress in steels. Using bainitic, martensitic, and stable austenitic steels, they demonstrated that transformation plasticity during the cooling of a uniaxially constrained specimen from the austenite phase field, acts to relieve the build up of thermal stress as the specimen cools. By contrast, the non-transforming austenitic steel exhibited a monotonic increase in residual stress with decreasing temperature, as might be expected from the thermal contraction of a constrained specimen. When the steels transformed to bainite or martensite, the transformation strain compensated for any thermal contraction strains that arose during cooling. Significant residual stresses were therefore found to build up only after transformation was completed, and the specimens approached ambient temperature (Fig. 8).

The experiments contain other revealing features. The thermal expansion coefficient of austenite ($1{\cdot}8 \times 10^{-6}$ K^{-1}) is much larger than that of ferrite ($1{\cdot}18 \times 10^{-6}$ K^{-1}), and yet the slope of the line before transformation is smaller when compared with that after transformation is completed (Fig. 8). This is because the austenite deforms plastically; its yield strength at high temperatures is reduced so much that the specimen is unable to accommodate the contraction strains elastically. Thus, the high temperature austenite part of each curve is virtually a plot of the yield strength as a function of temperature, as is evident from comparison with the actual yield strength data also plotted in Fig. 8*a*.

On the other hand, when ferrite forms, its strength at low temperatures is higher, so that the slope of the stress–temperature curve (after transformation is complete) should be steeper and consistent with the magnitude of thermal contraction strains. All this has yet to be incorporated into a quantitative model.

In the region of the stress–temperature curve where the transformation takes place, the interpretation of experimental data of the type illustrated in Fig. 8 is difficult. In the case of displacive transformations, the shape change due to transformation has a shear component which is much larger than the dilatational term (Table 1). This will give rise to significant intergranular microstresses, part of which will be relaxed plastically. This shear component will on average cancel out in a fine grained polycrystalline specimen containing plates in many orientations so that the average type II microstress component will be zero. However, the very nature of the stress effect is to favour the formation of selected variants,[75,76] in which case the shear component rapidly begins to dominate the transformation plasticity. Figure 8*a* shows that the stress can temporarily change sign as the specimen cools. This is because the stress selected variants continue to grow preferentially until transformation is exhausted.

Note that if transformation is completed at a higher temperature, then the ultimate level of stress at ambient temperature is larger, since the fully ferritic specimen contracts over a larger temperature range. To reduce the residual stress level at ambient temperature requires the design of alloys with low transformation temperatures. The types of high strength welding alloys used for making submarine hulls tend to have very low transformation temperatures ($<250^{\circ}$C). This fact may be fortuitous, but such alloys should be less susceptible to cracking induced by the development of macro residual stresses. Figure 9 illustrates one type of distortion found in welds, measured in terms of the angle θ through which the unconstrained plates rotate during the cooling to ambient temperature. Table 2 indicates how the distortion depends on the temperature at which the majority of the transformation is completed, for two manual metal arc welds deposited with a 60° V joint preparation in a multipass fabrication

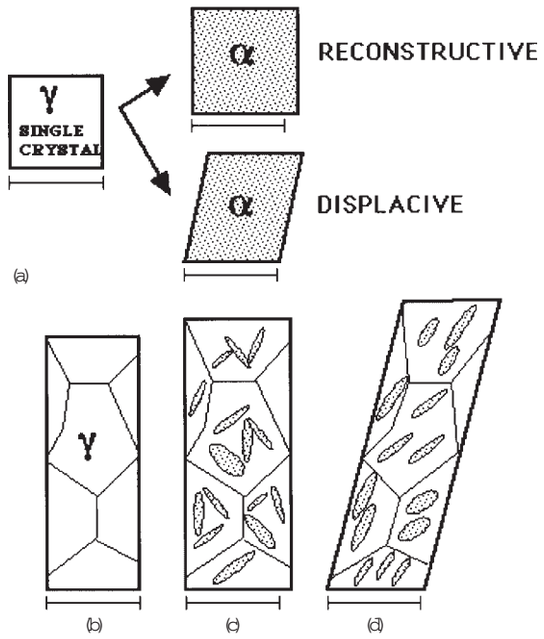

a two types of shape change that occur when single crystal of austenite transforms to single crystal of ferrite, as function of mechanism of transformation; *b* polycrystalline specimen of austenite; *c* polycrystalline specimen of austenite which has partially transformed by displacive transformation mechanism into random set of plates of ferrite; *d* polycrystalline specimen of austenite which has partially transformed by displacive transformation mechanism into organised set of plates of ferrite

7 Shape changes accompanying unconstrained transformation: note that horizontal scale bars are all of same length

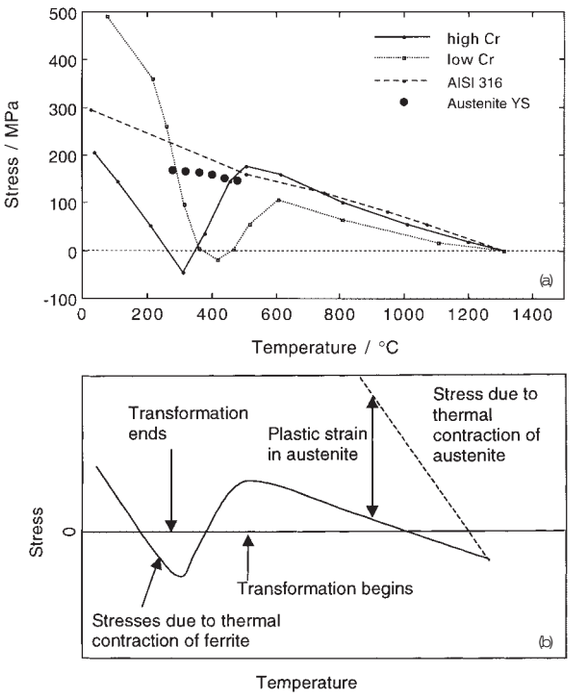

a axial macrostress that develops in uniaxially constrained specimens during cooling of martensitic (Fe–9Cr–1Mo), bainitic (Fe–2·5Cr–1Mo), and austenitic (AISI 316) steels[73,74] (also shown are some experimental data for YS of austenite in low alloy steel[75]); *b* schematic interpretation of Jones and Alberry[73,74] experiments

8 Role of transformations in development of residual stress in steels: thermal expansion coefficient of austenite is much larger than that of ferrite

involving about 11 layers with two beads per layer to complete the joint. The distortion is found to be significantly larger for the specimen where the transformation is completed at high temperatures.

ANISOTROPIC DEFORMATION

During their attempts to study the isothermal transformation of austenite using dilatometry, in 1930, Davenport and Bain[78] noticed that 'the volume change (due to transformation) is not necessarily uniformly reflected in a linear change in all dimensions'. In fact the thickness of flat disc specimens actually decreased as the volume increased. Recent work has demonstrated that in polycrystalline samples which are crystallographically textured, anisotropic transformation plasticity can be detected even in the absence of an applied stress.[79] When an unstressed polycrystalline sample of austenite is transformed, the shear components of the individual shape deformations of the large number of variants which form along any dimension should tend to cancel out on a large enough scale. Similarly, in the absence of stress, the dilatational component of the invariant-plane strain shape deformation should tend to average out so that the volume expansion appears to be isotropic.

Table 1 Shape change due to transformation: D and R denote displacive and reconstructive mechanisms respectively; invariant-plane strain here implies large shear component *s* as well as dilatational strain normal to the habit plane δ, values given are approximate and will vary slightly as function of lattice parameters and details of crystallography[71]

Transformation	Mechanism	Shape change	*s*	δ	Morphology
Iron alloys					
Allotriomorphic ferrite	R	Volume change	0	0·02	Irregular
Idiomorphic ferrite	R	Volume change	0	0·02	Equiaxed, faceted
Pearlite	R	Volume change	0	0·03	Spherical colonies
Widmanstätten ferrite	D	Invariant-plane strain	0·36	0·03	Thin plates
Bainite	D	Invariant-plane strain	0·22	0·03	Thin plates
Acicular ferrite	D	Invariant-plane strain	0·22	0·03	Thin plates
Martensite	D	Invariant-plane strain	0·24	0·03	Thin plates
Cementite plates	D and R	Invariant-plane strain?	0·21?	0·16?	Thin plates
Mechanical twins	D	Invariant-plane strain	$1/\sqrt{2}$	0	Thin plates
Annealing twins	R		0	0	Faceted
Cobalt					
Martensite	D	Invariant-plane strain	$1/(2\sqrt{2})$	0·01	Thin plates
Titanium					
Martensite	D	Invariant-plane strain	0·18	0·02	Thin plates
Hydride	D	Dilatation		0·18	Thin plates

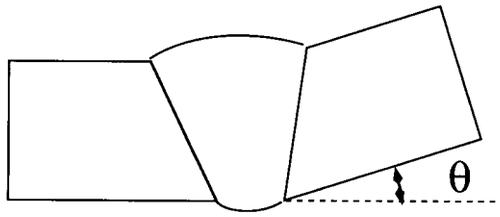

9 Example of distortion caused when pair of coplanar plates is welded together and joint is allowed to cool to ambient temperature

Transformation plasticity (the major component of which comes from the large shear strain of the invariant-plane strain) should therefore be smallest for a random polycrystalline sample, and due to volume change only. It is expected that in a crystallographically textured sample, the individual shear components of the shape deformations may not cancel out over large distances, thereby reducing their macroscopic effect. Transformation may then lead to anisotropic strains even in the absence of any applied stress.

Figure 10 shows a case where the application of a constant elastic stress biases the development of microstructure during the transformation of a steel to bainite.[80] The radial and longitudinal transformation strains then differ in sign and magnitude. To summarise, the observed plastic strain will be anisotropic when transformation occurs under the influence of stress. For reconstructive transformations, the extent of plasticity cannot exceed the volume strain, as long as the externally applied stress does not exceed the yield strength of the weaker phase. For displacive transformations, the plasticity can be much larger and more anisotropic when the microstructure becomes non-random.

MEASUREMENT OF MEAN PHASE TRANSFORMATION STRAINS

Diffraction is well suited to the monitoring of transformations and their related residual stresses. This is because the phase selectivity allows the tracking of both the extent of the transformation, through the integrated intensity of the transforming phase reflections, and the associated residual stress levels through the peak shifts. Neutron diffraction has the advantage that the transformation can be studied in the bulk, where the constraint is largest. This is well illustrated by the work of Vaidyananthan *et al.*[81] on the extent of the austenite to martensitic transformation as a function of temperature in superelastic Ni–Ti (Fig. 11).

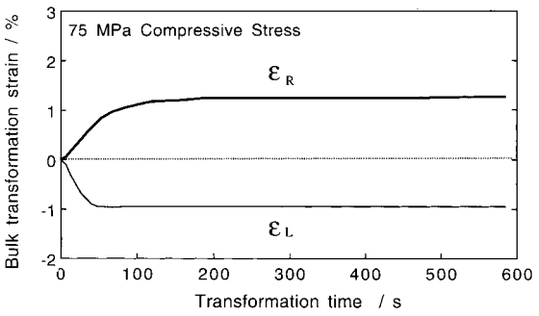

10 Development of anisotropic transformation strain when bainite forms under influence of constant, elastic applied compressive stress: note that shear strain associated with formation of one plate is of order of 26% with volume change of ~3%, potential for anisotropy is therefore much larger than illustrated here

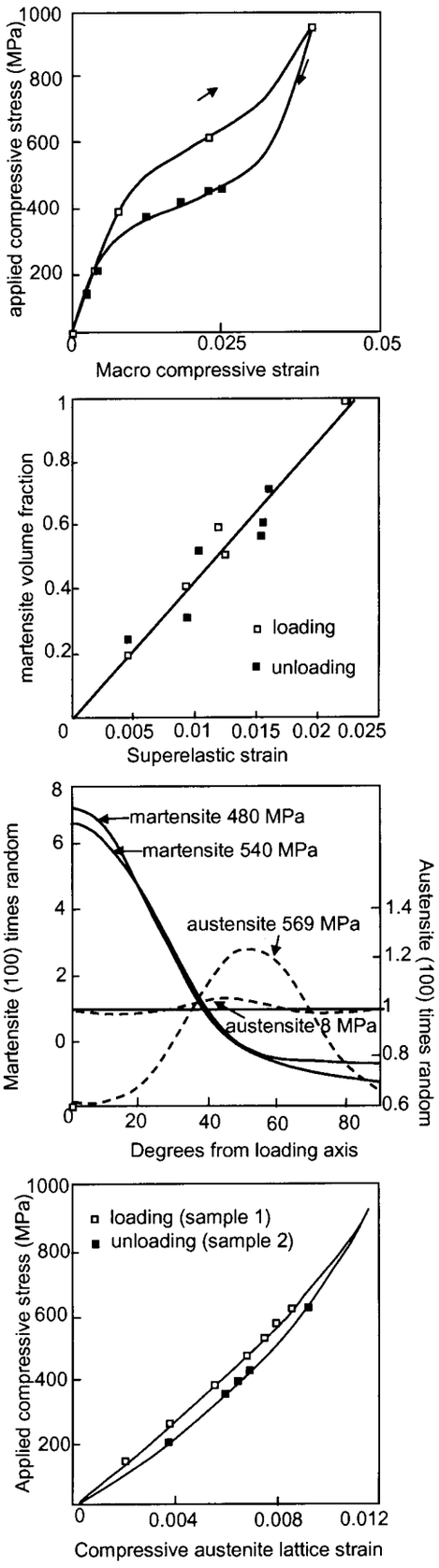

11 Extent of austenite to martensite transformation in Ni–Ti as function of strain measured by neutron diffraction: hysteresis of transformation is evident and is in part due to interaction between transformation and concomitant residual stress[81]

Table 2 Chemical compositions (wt-%), calculated transformation temperature range, and measured distortion θ for two manual metal arc, multipass weld deposits[77]

C	Si	Mn	Ni	Mo	Cr	ΔT, °C	θ, deg
0·06	0·5	0·9	…	…	…	802–400	14·5
0·06	0·3	1·6	1·7	0·4	0·35	422–350	8

Summary

Although residual stresses can have many different origins they are all the result of misfit. These misfits can be between different parts, different phases, or different regions within the same part. Furthermore, their origin can be mechanical, thermal, or plastic, or can arise from a transformation. Selection of the most appropriate methods for their measurement depends primarily upon the scale over which they act. In this overview, this has been defined in terms of the characteristic length l_0 over which the stress field self-equilibrates. No single method is capable of measuring across all the scales (type I, II, and III). Instead it is necessary to identify the scale most important to the property or suite of properties under consideration and to choose accordingly.

References

1. P. J. WITHERS and H. K. D. H. BHADESHIA: *Mater Sci. Technol.*, 2001, **17**, 355–365.
2. P. J. WITHERS: in 'Encyclopedia of materials science and technology', (ed. K. H. J. Buschow *et al.*), 2001, Oxford, Pergamon (to be published).
3. G. A. WEBSTER (ed.): 'Neutron diffraction measurements of residual stresses in a shrnk-fit ring and plug: a round robin study', VAMAS Report no. 38, Versailles Project on Advanced Materials and Standards, 2000, ISSN 1016–2186.
4. H. J. STONE, P. J. WITHERS, T. HOLDEN, S. M. ROBERTS, and R. C. REED: *Metall. Trans A*, 1998, **30A**, 1797–1808.
5. J. W. L. PANG, M. PREUSS, P. J. WITHERS, and G. J. BAXTER: Proc. 6th Int. Conf. on "Residule stresses', Oxford, UK, July 2000, (ed. G A. Webster), Vol. 2, 1415–1422; 2000, London, IoM Communications.
6. R. V. PRESTON, S. SMITH, H. R. SHERCLIFF, and P. J. WITHERS: *Sci. Technol. Weld. Join.*, to be published.
7. P. J. WEBSTER, L. DJAPIC OOSTERKAMP, P. A. BROWNE, D. J. HUGHES, W. P. KONG, P. J. WITHERS, and G. B. M. VAUGHAN: *J. Strain Anal. Eng. Des.*, 2001, to be published.
8. E. J. HEARN: 'Mechanics of materials', Vol. 2; 1985, Oxford, Pergamon.
9. G. S. SCHAJER, G. ROY, M. T. FLAMEN, and J. LU: in 'Handbook of measurement of residual stresses', (ed. J. Lu), 5–34; 1996, Lilburn, GA, Society for Experimental Mechanics.
10. D. Q. WANG, L. EDWARDS, I. B. HARRIS, and P. J. WITHERS: Proc. 4th European Conf. on 'Residual stresses' (ECRS4), Cluny, France, June 1996, (ed. S. Denis *et al.*), Vol. 1, 69–78; 1996, Paris, Société Française de Métallurgie et de Materiaux.
11. P. J. WEBSTER, G. MILLS, X. D. WANG, and W. P. KANG: Proc. 5th Int. Conf. on 'Residual stresses' (ICRS5), Linköping, Sweden, June 1997, (ed. T. Ericsson *et al.*), Vol. 1, 551–556; 1998, Linköping, Linköping Universitet.
12. J. F. FLAVENOT: in 'Handbook of measurement of residual stresses', (ed. J. Lu), 35–48; 1996, Lilburn, GA, Society for Experimental Mechanics.
13. L. PINTSCHOVIUS and V. JUNG: *Mater. Sci. Eng.*, 1983, **61**, 43–50.
14. J. H. FAUPEL: 'Engineering design'; 1981, Wiley, New York.
15. R. H. LEGGATT and T. G. DAVEY: in 'Mechanical relaxation of residual stresses', STP 993, 30–41; 1988, Philadelphia, PA, ASTM.
16. R. W. HERTZBERG: 'Deformation and fracture mechanics of engineering materials', 4th edn; 1996, New York, Wiley.
17. T. E. DAVIDSON, J. F. THROOP, and J. H. UNDERWOOD: 'Case histories in fracture mechanics', (ed. T. P. Rich and D. J. Cartwright), MS77-5, p. 3.9.1; 1977, US Army Materials Mechanics Research Centre.
18. L. PINTSCHOVIUS, E. MACHERAUCH, and B. SCHOLTES: *Mater. Sci. Eng.*, 1986, **84**, 163–170.
19. A. STACEY, H. J. MACGILLIVARY, G. A. WEBSTER, P. J. WEBSTER, and K. R. A. ZIBECK: *J. Strain Anal.*, 1985, **20**, 93–100.
20. M. PERL: *J. Pressure Vessel Technol. (Trans. ASME)*, 1998, **120**, 69–73.
21. G. C. JOHNSON: *J. Appl. Mech.*, 1981, **48**, 791–795.
22. R. H. LEGGATT: Proc. Int. Conf. on 'Stress relief heat treatment of welded structures', Sofia, Bulgaria, July 1987.
23. A. J. PERRY, J. A. SUE, and P. J. MARTIN: *Surf. Coat. Technol.*, 1996, **81**, 17–28.
24. E. GHEERAERT, A. DENEUVILLE, and A. M. BONNOT: *Diam. Relat. Mater.*, 1992, **1**, 525–528.
25. I. C. NOYAN, T. C. HUANG, and B. R. YORK: *Crit. Rev. Solid State Mater. Sci.*, 1995, **20**, 125–177.
26. T. W. CLYNE and S. C. GILL: *J. Therm. Spray Technol.*, 1996, **5**, (4), 1–18.
27. R. R. KIESCHKE, R. E. SOMEKH, and T. W. CLYNE: Proc. 3rd European Conf. on 'Composite materials', ECCM3, Bordeaux, France, (ed, A. R. Bunsell *et al.*), 265–272; 1989, Amsterdam, Elsevier.
28. S. KURODA and T. W. CLYNE: *Thin Solid Films*, 1991, **200**, 49–66.
29. R. W. HOFFMAN: in 'Physics of thin films', (ed. G. Hass and R. E. Thun), 211–273; 1966, New York, Academic Press.
30. P. BENGTSSON and C. PERSSON: *Surf. Coat. Technol.*, 1997, **92**, 78–86.
31. S. R. BROWN, I. G. TURNER, and H. REITER: *J. Mater. Sci.: Mater. Med.*, 1994, **5**, 756–759.
32. Y. C. TSUI and T. W. CLYNE: *Biomaterials*, 1997, **19**, 2015–2029.
33. S. G. MALHOTRA, Z. U. REK, S. M. YALISOVE, and J. C. BILELLO: *Thin Solid Films*, 1997, **301**, 45–54.
34. P. SCARDI, M. LEONI, and L. BERTAMINI: *Thin Solid Films*, 1996, **278**, 96–103.
35. P. SCARDI, M. LEONI, G. CAPPUCCIO, V. SESSA, and M. L. TERRANOVA: *Diam. Relat. Mater.*, 1997, **6**, 807–811.
36. D. PEIRO, J. BERTOMEU, F. ARRANDO, and J. ANDREU: *Mater. Lett.*, 1997, **30**, 239–243.
37. S. TADANO, M. TODOH, J. SHIBANO, and T. UKAI: *JSME Int. J. A: Mater. Eng.*, 1997, **40**, 328–335.
38. C. J. PICKUP, A. J. HORSEWELL, and P. J. WITHERS: *Acta Mater.*, 2001, to be published.
39. X. YANG and R. J. YOUNG: *Composites*, 1994, **25**, 488–493.
40. P. J. WITHERS: *Key Eng. Mater: Ceram. Matrix Compos.*, 1995, **108–110**, 291–314.
41. M. R. WATTS, P. J. WITHERS, M. E. FITZPATRICK, and A. M. KORSUNSKY: Proc. 4th European Conf. on 'Residual stresses' (ECRS4), Cluny, France, June 1996, (ed. S. Denis *et al.*), Vol. 2, 951–960; 1996, Paris, Société Française de Métallurgie et de Materiaux.
42. C. BALASINGH and V. SINGH: *Bull. Mater. Sci.*, 1997, **20**, 325–332.
43. S. M. PICKARD, D. B. MIRACLE, B. S. MAJUMDAR, K. L. KENDIG, L. ROTHENFLUE, and D. COKER: *Acta Metall. Mater.*, 1995, **43**, (8), 3105–3112.
44. J. D. ESHELBY: *Proc. R. Soc. A*, 1957, **241**, 376–396.
45. P. J. WITHERS, W. M. STOBBS, and O. B. PEDERSEN: *Acta Metall.*, 1989, **37**, 3061–3084.
46. T. W. CLYNE and P. J. WITHERS: in 'An introduction to metal matrix composites', Cambridge Solid State Series; 1993, Cambridge, Cambridge University Press.
47. K. K. CHAWLA: in 'Ceramic matrix composites', 1 edn, 416; 1993, London, Chapman and Hall.
48. D. HULL and T. W. CLYNE: 'An introduction to composite materials', Cambridge Solid State Science Series, (ed. D. R. Clarke *et al.*); 1996, Cambridge, Cambridge University Press.
49. M. E. FITZPATRICK, M. T. HUTCHINGS, and P. J. WITHERS: *Acta Mater.*, 1997, **45**, 4867–4876.
50. P. J. WITHERS, D. J. JENSEN, H. LILHOLT, and W. M. STOBBS: Proc. Conf. on 'Composite materials', ICCM6/ECCM2, (ed. F. L. Matthews *et al.*), 255–264; 1987; London, Elsevier.
51. P. J. WITHERS and A. P. CLARKE: *Acta Mater.*, 1998, **46**, 6585–6598.
52. R. I. TODD, M. A. M. BOURKE, C. E. BORSA, and R. J. BROOK: *Acta Metall. Mater.*, 1997, **45**, 1791–1800.
53. O. B. PEDERSEN and P. J. WITHERS: *Philos. Mag.*, 1992, **65**, 1217–1233.

54. J. LORCA, A. NEEDLEMAN, and S. SURESH: *Scr. Metall.*, 1990, **24**, 1203–1208.
55. Y. HUANG and R. J. YOUNG: *Compos. Sci. Technol.*, 1994, **52**, 505–517.
56. C. M. WEISBROOK and A. D. KRAWITZ: *Mater. Sci. Eng. A*, 1996, **209**, 318–328.
57. E. MAIRE, R. A. OWEN, J.-Y. BUFFIERE, and P. J. WITHERS: *Acta Mater.*, 2001, **49**, 153–163.
58. H. M. CLARK and C. M. WAYMAN: in 'Phase transformations', 59–114; 1970, Metals Park, OH, American Society for Metals.
59. J. W. CHRISTIAN: *Acta Metall.*, 1958, **6**, 377–379.
60. J. W. CHRISTIAN: *Metall. Trans. A*, 1982, **13A**, 509–538.
61. J. GOLDAK: in 'Recent trends in welding research', (ed. S. A. David and J. M. Vitek), 71–82; 1989, Materials Park, OH, ASM International.
62. L. TROIVE, L. KARLSSON, M. NASSTROM, P. WEBSTER, and K. S. LOW: in 'Recent trends in welding research', (ed. S. A. David and J. M. Vitek), 107–112; 1989, Materials Park, OH, ASM International.
63. S. SJOSTROM: *Mater. Sci. Technol.*, 1985, **1**, 823–829.
64. J. B. LEBLOND and J. DEVAUX: Proc. 2nd Int. Conf. on 'Residual stresses', Nancy, France, 410–415; 1989, New York, Elsevier.
65. J. B. LEBLOND, G. MOTTET, and J. C. DEVAUX: *J. Mech. Phys. Solids*, 1986, **34**, 395–409; 411–432.
66. J. B. LEBLOND, G. MOTTET, and J. C. DEVAUX: *Int. J. Plast.*, 1989, **5**, 551–572.
67. J. B. LEBLOND: *Int. J. Plast.*, 1989, **5**, 573–591.
68. J. B. LEBLOND: Internal Report, FRAMASOFT, Paris, CSS/L/NT/90/4022, 1990.
69. H. K. D. H. BHADESHIA: in 'Mathematical modelling of weld phenomena 2', (ed. H. K. D. H. Bhadeshia), 71–118; 1995, London, Institute of Materials.
70. J. W. CHRISTIAN: 'Physical properties of martensite and bainite', 1965, London, The Iron and Steel Institute.
71. H. K. D. H. BHADESHIA: 'Worked examples in the geometry of crystals'; 1987, London, The Institute of Materials.
72. J. S. BOWLES and J. K. MACKENZIE: *Acta Metall.*, 1954, **2**, 129–137.
73. W. K. C. JONES and P. J. ALBERRY: in 'Ferritic steels for fast reactor steam generators', 1–4; 1977, London, British Nuclear Engineering Society.
74. W. K. C. JONES and P. J. ALBERRY: in 'Residual stresses in welded constructions'; 1977, Cambridge, The Welding Institute.
75. P. H. SHIPWAY and H. K. D. H. BHADESHIA: *Mater. Sci. Eng. A*, 1995, **A201**, 143–149.
76. C. L. MAGEE: 'Transformation kinetics, microplasticity and aging of martensite', PhD thesis, Carnegie Mellon University, 1966.
77. H. K. D. H. BHADESHIA and L. E. SVENSSON: unpublished research, Department of Materials Science and Metallurgy, University of Cambridge, 1994.
78. E. S. DAVENPORT and E. C. BAIN: *Trans. AIME*, 1930, **90**, 117–154.
79. H. K. D. H. BHADESHIA, S. A. DAVID, J. M. VITEK, and R. W. REED: *Mater. Sci. Technol.*, 1991, **7**, 686–698.
80. A. MATSUZAKI, H. K. D. H. BHADESHIA, and H. HARADA: *Acta Metall. Mater.*, 1994, **42**, 1081–1090.
81. R. VAIDYANATHAN, M. A. M. BOURKE, and D. C. DUNAND: *Acta Mater.*, 1999, **37**, 3353–3366.